HHS Public Access

Author manuscript

Cornea. Author manuscript; available in PMC 2021 May 01.

Published in final edited form as:

Cornea. 2020 May ; 39(5): 598–604. doi:10.1097/ICO.0000000000002232.

Application of Corneal Optical Coherence Tomography Angiography for Assessment of Vessel Depth in Corneal Neovascularization

Afshan Nanji, MD MPH[1,†], **Travis Redd, MD MPH**[1,2,†], **Winston Chamberlain, MD PhD**[1], **Julie M. Schallhorn, MD**[2], **Siyu Chen, PhD**[3], **Stefan Ploner, MS**[3,4], **Andreas Maier, PhD**[4], **James G. Fujimoto, PhD**[3], **Yali Jia, PhD**[1], **David Huang, MD PhD**[1], **Yan Li, PhD**[1]

[1.]Casey Eye Institute, Oregon Health & Science University, Portland, OR, USA.

[2.]Department of Ophthalmology, University of California San Francisco, San Francisco, CA, USA.

[3.]Department of Electrical Engineering & Computer Science and Research Laboratory of Electronics, Massachusetts Institute of Technology, Cambridge, MA, USA.

[4.]Pattern Recognition Lab and SAOT, University Erlangen Nuremberg, Erlangen, Germany.

Abstract

Purpose: To map and measure the depths of corneal neovascularization (NV) using 3-dimensional optical coherence tomography angiography (OCTA) at two different wavelengths.

Methods: Corneal NV of varying severity, distribution, and underlying etiology was examined. Average NV depth and vessel density were measured using 840-nm spectral-domain OCTA and 1050-nm swept-source OCTA. The OCTA results were compared to clinical slit-lamp estimation of NV depth.

Results: 12 eyes with corneal NV from 12 patients were imaged with OCTA. Clinically “superficial”, “mid-stromal”, and “deep” cases had an average vessel depth of 23%, 39%, and 66% depth on 1050-nm OCTA, respectively. Average vessel depth on OCTA followed a statistically significant ordinal trend according to clinical classification of vessel depth (Jonckheere-Terpstra test, $p<0.001$). In 8 cases where both 840-nm OCTA and 1050-nm OCTA were acquired, there was excellent agreement in the mean vessel depth between the two systems (concordance correlation coefficient=0.94, $p<0.001$). The average vessel density measured by 840-nm OCTA was higher (average 1.6-fold) than that measured by 1050-nm OCTA.

Conclusion: Corneal OCTA was able to map corneal NV in three-dimensions, measure vessel depth and density. The depth of corneal NV varied between different pathologies in a manner

Correspondence to: Yan Li, PhD, address: 3375 SW Terwilliger Blvd, Portland, OR 97239 Tel: 503-494-6394, Fax: 503-494-3929, liyan@ohsu.edu.

[†]Authors sharing first co-authorship

Conflicts of Interest and Source of Funding:

Oregon Health & Science University (OHSU), Y.L., Y.J., and D.H. have a significant financial interest in Optovue, Inc, a company that may have a commercial interest in the results of this research and technology. These potential conflicts of interest have been reviewed and managed by OHSU. J.G.F. received royalties from intellectual property owned by MIT and licensed to Optovue, Inc. and Carl Zeiss Meditec, Inc. The other authors have no proprietary or commercial interest in the materials discussed in this article.

consistent with prior pathologic studies. The measured vessel density appeared to be affected by the inter-scan time, which affects blood flow velocity sensitivity, and the wavelength, which affects the ability to penetrate through opacity. These findings suggest possible clinical applications of OCTA for the diagnosis of corneal pathology, and quantitative monitoring of therapeutic response in corneal NV patients.

Keywords

Corneal neovascularization; optical coherence tomography angiography; vessel depth; vessel density

INTRODUCTION

Corneal neovascularization (NV) is the pathologic infiltration of blood vessels into an otherwise clear matrix of the cornea, resulting from a disruption in the balance between pro- and anti-angiogenic factors.[1, 2] It develops from a variety of causes including infections, immunologic processes, surgery, and trauma.[3, 4] These vessels may then lead to corneal edema, exudation of lipid, and corneal scarring, thus decreasing vision; they also compromise the immune privilege status of the cornea, and in cases of NV into corneal grafts, increase the risk of graft rejection.[5]

Traditional methods to evaluate corneal NV include slit-lamp biomicroscopy and color photography or videography;[6, 7] however, these have significant shortcomings including imprecision, lack of quantification, difficulty of vessel delineation in areas of scarring,[8] and inability to assess blood flow.[9] Corneal angiography, specifically fluorescein angiography (FA) and indocyanine green angiography (ICGA), offers improvements in the detailed visualization of vessels, blood flow timing, and direction, even in the presence of corneal scarring.[10] These techniques have been used for diagnostic purposes and to monitor response to treatment of corneal NV.[9] However, FA and ICGA are time-intensive, invasive, and carry a small risk of systemic adverse reaction, limiting their practical utility in the clinical setting.[11, 12] In light of this, non-invasive imaging modalities for corneal NV are needed.[13]

More recently, optical coherence tomography (OCT) angiography (OCTA) has undergone preliminary evaluation as a method of imaging corneal NV.[14–18] OCTA takes advantage of the high scan speed of Fourier-domain OCT for angiographic imaging, and uses motion contrast to detect flow within blood vessels. Erythrocyte movement within vessels is detected by comparing sequential OCT cross-sectional scans.[19–21] This technology has experienced a rapid expansion in its applicability to the anterior segment in recent years.[22, 23] However, to date, corneal OCTA has been evaluated primarily in an *en face* orientation, providing a projection map of corneal NV.[15, 16] This only partially utilizes the 3-dimensional (3D) volumetric data in OCTA and leaves out potentially valuable diagnostic information. Mapping and quantifying vessel depth and density would capture this diagnostic information, facilitating inter-subject comparison for diagnostic classification and serial intra-subject measurement to monitor treatment response. This article describes an exploratory use of OCTA for quantitative *in vivo* assessment of the depth and density of

corneal NV in a variety of conditions. Moreover, in this study, we used and compared two imaging systems, a 1050-nm swept-source research OCT prototype and an 840-nm spectral-domain commercially available OCT scanner.

METHODS

This study adhered to the tenets of the Declaration of Helsinki and was in accord with the Health Insurance Portability and Accountability Act of 1996. The study protocol was approved by the Institutional Review Board of Oregon Health & Science University. Clinical trial registration was not required due to the observational nature of the study. Written informed consent was obtained from all study participants.

Subject Selection and Image Acquisition

Eligible participants were corneal NV patients seen at Casey Eye Institute. Patients were first evaluated by clinicians. Depth of NV in the cornea was categorized clinically at the slit lamp using the brightest lamp illumination and high (16x) magnification with angled narrow slit beam. An ordinal category of “superficial”, “mid-stromal”, or “deep” was assigned if a majority of the vessels were found in the anterior 25%, mid 25 to 75%, or posterior 25% of the cornea, respectively. Patients were then imaged using both a prototype swept-source OCTA system and a commercially available spectral-domain OCTA system (Avanti with AngioVue and a corneal adapter module, Optovue Inc., Fremont, CA).

The swept-source OCTA system has a central wavelength of 1050nm, performs 100,000 axial-scans per second, has an axial resolution of 7 μm and a focal spot size of 22 μm ($1/e^2$ intensity diameter). 3D horizontal and vertical OCTA raster data consisting of 300 by 300 axial-scans was acquired over a square region (either 6×6 mm^2 or 9×9 mm^2 in size) with a scan depth of 5 mm in tissue. Three repeated cross-sectional scans were captured at each location. Subpixel precision pre-registration between repeated B-scans was performed before OCTA calculations to reduce line artifacts caused by in-plane motion. The split-spectrum amplitude-decorrelation angiography (SSADA) algorithm was used to calculate the flow signal.[21] Flow was measured by the decorrelation between repeated B-scans. The inter-scan time was 3.3 msec including the time to perform the B-scan and the flyback (between two consecutive B-scans). Orthogonal registration was performed to merge one horizontal and one vertical raster scans into a single volume.[24, 25]

The spectral-domain OCTA system has a central wavelength of 840 nm, performs 70,000 axial-scans per second, has an axial resolution of 5μm and a focal spot size of 15.5μm. The AngioVue OCTA scan pattern is a 3D volumetric angiography scan consisting of 304 by 304 axial-scans to cover a square area. The nominal imaging area was either 3×3 mm^2 or 6×6 mm^2 in the retina, which translated to 4.5×4.5 mm^2 or 9×9 mm^2 for cornea scanning with the anterior segment adaptor lens. The image depth is 2 mm in tissue. Two repeated cross-sectional scans were captured at each location before proceeding to the next position. The inter-scan time was 4.8 msec. The AngioVue also uses SSADA algorithm and orthogonal registration (commercially called *motion correction technology or MCT*).

Custom regression-based algorithms were used to estimate decorrelation signal caused by eye motion and subtract this artifact from the OCTA image. This bulk-motion subtraction algorithm is essential to distinguish blood flow from artifacts due to saccades or other eye motions. It is similar to one published for correcting retinal OCTA.[26]

Measuring Neovascularization Parameters

The anterior and posterior corneal surfaces were segmented in cross-sectional OCT structure images.[27] The *en face* OCT structure image was calculated by averaging reflectance between the two corneal boundaries. The *en face* corneal angiogram was constructed by projecting the maximal flow signal between corneal boundaries (Figure 1). Then a region of interest (ROI) was manually delineated on the *en face* OCTA by one corneal specialist (W.C.) according to the clinically identified region of corneal NV. The value of each *en face* OCTA pixel was compared with a threshold value (99 percentile OCTA flow signal of normal corneas) to generate a binary vessel mask (Figure 1). White pixels in the vessel mask indicate vessels of interest. Pixels outside the ROI and non-vessel pixels inside the ROI were both set to black. The vessel density was calculated as the percentage of the ROI (marked by red lines) occupied by vessels (marked by white pixels) on OCTA *en face* vessel mask (Figure 1).[28] The vessel densities acquired by 840-nm and 1050-nm OCTA were then compared by taking the ratios of the two measurements.

Cross-sectional OCT angiograms were used to determine the depth of blood vessels inside the tissue. Blood vessels were located by OCTA (projection resolved flow signal marked vessels in red on cross-sectional OCTA) inside the tissue. The vessel depth was calculated as the distance from the anterior corneal surface to the blood vessel (Figure 1). A percentage (%) vessel depth was also calculated as the vessel depth divided by the total corneal thickness at that location. Superficial (anterior 25%, blue), mid-stromal (25~75%, green), or deep (posterior 25%, red) corneal vessels were illustrated using different colors in vessel depth maps (Figures 1–3). For each cornea, vessel depth measurements in micron and percentage were averaged over the corneal NV ROI. Custom algorithms developed with MATLAB R2017a software (The Math Works, Inc.; Natick, MA, USA) was used to segment corneal boundaries, measure corneal NV vessel density and vessel depth. The percentage vessel depth was compared with the ordinal clinical depth classification using the Jonckheere-Terpstra test. The average percent vessel depth and density measurements by 840-nm and 1050-nm OCTA were compared using the Lin's concordance correlation coefficient and the paired sample t-test. A p-value less than 0.05 was considered statistically significant. Descriptive statistics and other statistical analysis was performed using Stata MP 13 (StataCorp, College Station, TX).

RESULTS

Twelve eyes (9 right eyes and 3 left eyes) with corneal NV from 12 patients were imaged with OCTA; participants' ages ranged from 23 to 85 years, with 7female and 5 male (Table). Five patients had interstitial keratitis, 2 had limbal stem cell deficiency, 3 were cases of corneal transplant rejection, one was a pterygium, and one was a neurotrophic ulcer.

According to clinical examination, four cases had superficial corneal NV, four had mid-stromal NV, and four had deep NV (Table).

Cases with NV classified as “superficial” by clinical exam had an overall average vessel depth on OCTA of 23% corneal thickness (95% confidence interval [CI]: 4–42%, range: 16–41%), clinically “mid-depth” cases averaged 39% depth on OCTA (95% CI 24–53%, range: 30–49%), and clinically “deep” cases averaged 66% depth on OCTA (95% CI: 53–79%, range: 60–78%) using the 1050-nm OCTA. Average vessel depth on OCTA followed a statistically significant ordinal trend according to clinical classification of vessel depth (Jonckheere-Terpstra test, $p<0.001$).

Among 5 cases diagnosed with interstitial keratitis, the overall average vessel depth was 47% (range: 16–65%). Interestingly, both cases of interstitial keratitis attributable to varicella zoster virus (VZV) demonstrated relatively superficial NV (16 and 32% average depth), whereas the two cases attributable to herpes simplex virus (HSV) demonstrated deeper NV (60 and 62% average depth). One case of limbal stem cell deficiency in the setting of penetrating keratoplasty demonstrated superficial NV (Case 6; 16% average vessel depth), while the other case of limbal stem cell deficiency due to Stevens Johnson syndrome and corneal conjunctivalization demonstrated mid-stromal NV (Case 7; 41% average vessel depth). All three cases of NV due to corneal transplant stromal rejection (1 deep anterior lamellar keratoplasty, 2 penetrating keratoplasties) demonstrated mid-stromal NV (Cases 8, 9, and 10; average depths of 30%, 44%, and 49%, respectively). The pterygium showed superficial NV (19% average depth), as expected. The one case of neurotrophic ulcer showed deep NV (78% average depth). Example OCTA images of interstitial keratitis, stem cell deficiency, and pterygium are depicted in Figure 2.

In 8 cases, both 840-nm and 1050-nm OCTA scans were obtained. The vessel depth and vessel density calculations for these scans were compared in the Table. There was high agreement in the mean vessel depth among the 8 cases between spectral-domain and swept-source OCTA (Lin’s concordance correlation coefficient = 0.94, $p<0.001$). No statistical significant difference was found between the average vessel depth of the two OCTA (paired t-test $p=0.14$). The greatest discrepancy occurred in the case of idiopathic interstitial keratitis (Case 5; mean vessel depth was 51% of the total corneal thickness according to 840-nm OCTA, and 65% according to the 1050-nm OCTA). Figure 3 provides a visual comparison of 840-nm and 1050-nm OCTA on a neurotrophic ulcer case and a transplant rejection case. Figure 4 demonstrates that vessels without flow (“ghost vessels”) were not imaged by OCTA.

The overall average vessel density was measured to be 33% (95% CI: 14–52%, range: 8–70%) with 840-nm OCTA and 27% (95% CI: 13–41%, range: 4–59%) with 1050-nm OCTA. The agreement in vessel density between spectral-domain and swept-source OCTA was poor (Lin’s concordance correlation coefficient=0.53, $p=0.11$) but no statistically significant difference was detected (paired t-test $p=0.40$). On average, 840-nm OCTA measured higher vessel density (mean ± standard deviation: 1.6±1.4 fold) than 1050-nm OCTA. However, in one case of deep NV with significant corneal scarring (case 12, Figure 3 top), the longer

wavelength 1050-nm OCTA measured 3-fold higher vessel density than the shorter wavelength 840-nm OCTA.

The bulk motion suppression algorithm was applied to all scans, and its effect in reducing motion artifact is demonstrated in Figure 5.

Scans were obtained 3 times consecutively on Case 7 to assess measurement repeatability with the 1050-nm OCTA system. Standard deviations from these measurements were 1.6 μm for mean vessel depth (coefficient of variation [CV]=0.8%) and 2.1% for vessel density (CV=7.2%).

DISCUSSION

This exploratory study describes the use of *en face* and volumetric OCTA to evaluate corneal neovascularization in three-dimensions, and compares the depth of corneal NV among several different etiologies. Key findings include: 1) Corneal OCTA is able to precisely image corneal NV in three-dimensions with reduced motion artifact and strong agreement with clinical estimation of vessel depth; 2) Depth of corneal NV varied among different pathologic processes in a manner consistent with prior pathologic studies; 3) Spectral-domain and swept-source OCTA scans provided similar estimates of corneal NV depth; and 4) On average, slower scanning spectral-domain OCTA gave higher vessel density measurements than the faster scanning swept-source OCTA. These findings are useful to inform future studies for development and validation of 3-dimensional corneal OCTA imaging, and suggest potential clinical applications both for diagnosis and quantitative monitoring of therapeutic response in patients with corneal NV.

This study represents the first application of corneal OCTA to quantify depth of corneal NV. The results demonstrate that OCT angiography is capable of differentiating vessel depth in corneal NV, and can provide an estimated average vessel depth, which corresponded well to the clinical examination. The system only detects vessels with active flow (Figure 4), and thus may help differentiate active from quiescent disease. We have also employed a novel bulk motion suppression algorithm to reduce artifact caused by eye motion, which improves image quality (Figure 5). The obvious benefit of an OCTA system such as this over clinical examination is that it allows quantification of both the 3-dimensional extent and overall density of corneal NV, which provides more information than subjective assignment to an ordinal category (i.e. “superficial,” “mid-stromal,” or “deep”). Parameters such as average vessel depth, total area of NV, and NV density could be followed over time to monitor clinical course and response to treatment.[16]

Different underlying etiologies of corneal NV appeared to be associated with different depths of NV on corneal OCTA in this study, and in a manner consistent with prior histologic examinations of similar conditions.[29–32] Specifically, the two cases of interstitial keratitis due to HSV reported here demonstrated deep NV, whereas those due to VZV had mid-stromal or superficial NV. Pathologic studies have demonstrated that HSV is classically associated with deeper NV due to a presumed antigenic response to Descemet’s membrane.[4] One limbal stem cell deficiency case (Case 6) demonstrated mostly superficial NV, which is

consistent with the known pathology of this condition.[3] The other limbal stem cell deficiency case due to Stevens Johnson syndrome and corneal conjunctivalization (Case 7, Figure 2 middle row) had a superficial component of NV near the limbus and a mid-stromal component of NV towards the central cornea. The vessel depth averaged to 31–41% in that eye. Finally, the three cases of corneal transplant stromal rejection showed mostly mid-stromal NV, which is consistent with histologic findings in similar cases.[29] However, it should be noted that a detailed catalogue of typical NV depth for various angiogenic conditions in the cornea does not exist, even in the pathology literature. Corneal OCTA provides an excellent opportunity to address this knowledge gap, as it provides precise quantification of vessel depth, does not require removal of the tissue in question, provides an *in vivo* assessment of vessel depth without potential confounding from tissue processing effects, includes only active NV and not ghost vessels, and is repeatable in the same specimen, allowing longitudinal assessment over time. Establishment of a robust database describing the depth, distribution, and density of NV for various pathologic processes may allow the clinical application of corneal OCTA in the future to aid diagnosis of idiopathic corneal NV. Of note, the cases presented here represent corneal NV in inflammatory, infectious, and degenerative conditions. Corneal OCTA findings in other disease categories, such as congenital and neoplastic etiologies, warrant investigation in future studies.[2]

Two imaging systems were compared in this study: 1050-nm swept-source OCTA, which is used primarily in research settings and provides deeper penetration by acquiring images, and 840-nm spectral-domain OCTA, which is commercially-available. Both have independently been evaluated for corneal NV, but their results have never been directly compared.[16, 18, 33]

We found a very strong correlation in the estimated average vessel depth between these two systems, suggesting that either may be suitable for assessing depth of corneal NV.

The average vessel density measured by 840-nm spectral-domain OCTA was higher than that measured by 1050-nm swept-source OCTA. The one exception was the case of deep NV with corneal scarring, in which the longer wavelength OCTA measured higher vessel density. There are several reasons may lead to the difference in vessel density measurements. First, the two systems have different inter-scan time (interval between B-scans). In this study, the spectral domain OCTA has a longer inter-scan time than that of the swept-source OCTA (4.8 msec vs. 3.3 msec). Longer inter-scan time are more sensitive to slow blood flow.[20, 34] Thus the longer inter-scan time employed by the 840-nm spectral-domain OCTA may allow it to detect a greater percentage of capillaries that have slow flow velocities. Second, the longer wavelength 1050-nm OCTA provides better penetration than the 840-nm OCTA. 840-nm OCTA may not be adequate to detect deep NV with the presence of dense corneal scarring (Figure 3 top). Third, the scan areas of the two systems were not completely overlap due to differences in scan size, scan positioning, and patient fixation (some patients had poor vision).

This study has several limitations. First, repeat scans were obtained in only one case, and while these results did indicate high repeatability of measurements, a larger sample size is required to validate repeatability. Second, clinical diagnosis was based on examination findings and clinical course; there was no pathologic verification of underlying diagnosis.

However, diagnoses were all made by corneal subspecialists, and pathologic verification of the diagnosis would not have been feasible or warranted in most cases. Third, delineation of the *en face* extent of NV was performed manually. Fourth, clinical estimation of vessel depth was based on the examining provider's judgment, and may vary among different providers. Finally, lymphangiogenesis likely plays an important role in the pathology associated with corneal NV, particularly with respect to immune rejection; however, lymphatic fluid is clear and lack blood cells to provide backscattered OCT signal to be depicted by current OCTA techniques, and thus is not assessed in this study. Future development of OCTA system may provide wider OCTA scans or montage multiple scans to report maximal extent of NV onto the cornea (either distance from the limbus or from the corneal apex). Future studies involving a larger cohort with serial imaging of cases over time are warranted to further evaluate OCTA for assessing corneal NV.

In summary, this study describes the use of volumetric corneal OCTA to evaluate the distribution of corneal NV in three dimensions. We found high concordance of average vessel depth as measured by OCTA with clinical estimation of NV depth. Characteristic depths of NV also appeared to be associated with different disease processes, which is consistent with prior histologic studies. These findings suggest potential utility for this or similar systems in diagnosis and therapeutic monitoring of patients with corneal NV, and inform future studies of this technology.

Acknowledgments

This study was supported by the National Institutes of Health, Bethesda, MD (grants: R01EY028755, R01EY029023, R01EY011289, R01EY027833, R01EY024544, P30EY010572); a research grant and equipment support from Optovue, Inc., Fremont, CA; unrestricted grants to Casey Eye Institute from Research to Prevent Blindness, Inc., New York, NY. The sponsors did not participate in the data collection, data management, or data analysis in the present study.

REFERENCES

1. Doggart JH. Vascularization of the cornea. Br J Ophthalmol 1951;35:160–7. [PubMed: 14821291]
2. Chang JH, Gabison EE, Kato T, Azar DT. Corneal neovascularization. Curr Opin Ophthalmol 2001;12:242–9. [PubMed: 11507336]
3. Abdelfattah NS, Amgad M, Zayed AA, et al. Clinical correlates of common corneal neovascular diseases: a literature review. Int J Ophthalmol 2015;8:182–93. [PubMed: 25709930]
4. Di Zazzo A, Kheirkhah A, Abud TB, et al. Management of high-risk corneal transplantation. Surv Ophthalmol 2017;62:816–27. [PubMed: 28012874]
5. Volker-Dieben HJ, D'Amaro J, Kok-van Alphen CC. Hierarchy of prognostic factors for corneal allograft survival. Aust N Z J Ophthalmol 1987;15:11–8. [PubMed: 3297110]
6. Conrad TJ, Chandler DB, Corless JM, Klintworth GK. In vivo measurement of corneal angiogenesis with video data acquisition and computerized image analysis. Lab Invest 1994;70:426–34. [PubMed: 7511717]
7. Bock F, Onderka J, Hos D, et al. Improved semiautomatic method for morphometry of angiogenesis and lymphangiogenesis in corneal flatmounts. Exp Eye Res 2008;87:462–70. [PubMed: 18789928]
8. Spiteri N, Romano V, Zheng Y, et al. Corneal angiography for guiding and evaluating fine-needle diathermy treatment of corneal neovascularization. Ophthalmology 2015;122:1079–84. [PubMed: 25841974]
9. Steger B, Romano V, Kaye SB. Corneal Indocyanine Green Angiography to Guide Medical and Surgical Management of Corneal Neovascularization. Cornea 2016;35:41–5. [PubMed: 26555579]

10. Kirwan RP, Zheng Y, Tey A, et al. Quantifying changes in corneal neovascularization using fluorescein and indocyanine green angiography. Am J Ophthalmol 2012;154:850–8 e2. [PubMed: 22840481]
11. Kwiterovich KA, Maguire MG, Murphy RP, et al. Frequency of adverse systemic reactions after fluorescein angiography. Results of a prospective study. Ophthalmology 1991;98:1139–42. [PubMed: 1891225]
12. Stanga PE, Lim JI, Hamilton P. Indocyanine green angiography in chorioretinal diseases: indications and interpretation: an evidence-based update. Ophthalmology 2003;110:15–21; quiz 2–3. [PubMed: 12511340]
13. Cursiefen C, Colin J, Dana R, et al. Consensus statement on indications for antiangiogenic therapy in the management of corneal diseases associated with neovascularisation: outcome of an expert roundtable. Br J Ophthalmol 2012;96:3–9. [PubMed: 21712359]
14. Ang M, Devarajan K, Das S, et al. Comparison of anterior segment optical coherence tomography angiography systems for corneal vascularisation. Br J Ophthalmol 2018;102:873–7. [PubMed: 28939690]
15. Ang M, Cai Y, Shahipasand S, et al. En face optical coherence tomography angiography for corneal neovascularisation. Br J Ophthalmol 2016;100:616–21. [PubMed: 26311064]
16. Ang M, Sim DA, Keane PA, et al. Optical Coherence Tomography Angiography for Anterior Segment Vasculature Imaging. Ophthalmology 2015;122:1740–7. [PubMed: 26088621]
17. Cai Y, Alio Del Barrio JL, Wilkins MR, Ang M. Serial optical coherence tomography angiography for corneal vascularization. Graefes Arch Clin Exp Ophthalmol 2017;255:135–9. [PubMed: 27722920]
18. Ang M, Cai Y, Tan AC. Swept Source Optical Coherence Tomography Angiography for Contact Lens-Related Corneal Vascularization. J Ophthalmol 2016;2016:9685297. [PubMed: 27752366]
19. Wang RK. Optical Microangiography: A Label Free 3D Imaging Technology to Visualize and Quantify Blood Circulations within Tissue Beds in vivo. IEEE J Sel Top Quantum Electron 2010;16:545–54. [PubMed: 20657761]
20. Choi W, Moult EM, Waheed NK, et al. Ultrahigh-Speed, Swept-Source Optical Coherence Tomography Angiography in Nonexudative Age-Related Macular Degeneration with Geographic Atrophy. Ophthalmology 2015;122:2532–44. [PubMed: 26481819]
21. Jia Y, Tan O, Tokayer J, et al. Split-spectrum amplitude-decorrelation angiography with optical coherence tomography. Opt Express 2012;20:4710–25. [PubMed: 22418228]
22. Ang M, Baskaran M, Werkmeister RM, et al. Anterior segment optical coherence tomography. Prog Retin Eye Res 2018;66:132–56. [PubMed: 29635068]
23. Spaide RF, Fujimoto JG, Waheed NK, et al. Optical coherence tomography angiography. Prog Retin Eye Res 2018;64:1–55. [PubMed: 29229445]
24. Kraus MF, Potsaid B, Mayer MA, et al. Motion correction in optical coherence tomography volumes on a per A-scan basis using orthogonal scan patterns. Biomed Opt Express 2012;3:1182–99. [PubMed: 22741067]
25. Kraus MF, Liu JJ, Schottenhamml J, et al. Quantitative 3D-OCT motion correction with tilt and illumination correction, robust similarity measure and regularization. Biomed Opt Express 2014;5:2591–613. [PubMed: 25136488]
26. Camino A, Jia Y, Liu G, et al. Regression-based algorithm for bulk motion subtraction in optical coherence tomography angiography. Biomed Opt Express 2017;8(6):3053–66. [PubMed: 28663926]
27. Li Y, Shekhar R, Huang D. Corneal pachymetry mapping with high-speed optical coherence tomography. Ophthalmology 2006;113(5):792–9 e2. [PubMed: 16650675]
28. Skalet AH, Li Y, Lu CD, et al. Optical Coherence Tomography Angiography Characteristics of Iris Melanocytic Tumors. Ophthalmology 2017;124(2):197–204. [PubMed: 27856029]
29. Cursiefen C, Kuchle M, Naumann GO. Angiogenesis in corneal diseases: histopathologic evaluation of 254 human corneal buttons with neovascularization. Cornea 1998;17(6):611–3. [PubMed: 9820941]
30. Chang JH, Garg NK, Lunde E, et al. Corneal neovascularization: an anti-VEGF therapy review. Surv Ophthalmol 2012;57(5):415–29. [PubMed: 22898649]

31. Tshionyi M, Shay E, Lunde E, et al. Hemangiogenesis and lymphangiogenesis in corneal pathology. Cornea 2012;31(1):74–80. [PubMed: 22030600]

32. Ellenberg D, Azar DT, Hallak JA, et al. Novel aspects of corneal angiogenic and lymphangiogenic privilege. Prog Retin Eye Res 2010;29(3):208–48. [PubMed: 20100589]

33. Chan SY, Pan CT, Feng Y. Localization of corneal neovascularization using optical coherence tomography angiography. Cornea 2019;38(7):888–95. [PubMed: 30908339]

34. Moult E, Choi W, Waheed NK, et al. Ultrahigh-speed swept-source OCT angiography in exudative AMD. Ophthalmic Surg Lasers Imaging Retina 2014;45(6):496–505. [PubMed: 25423628]

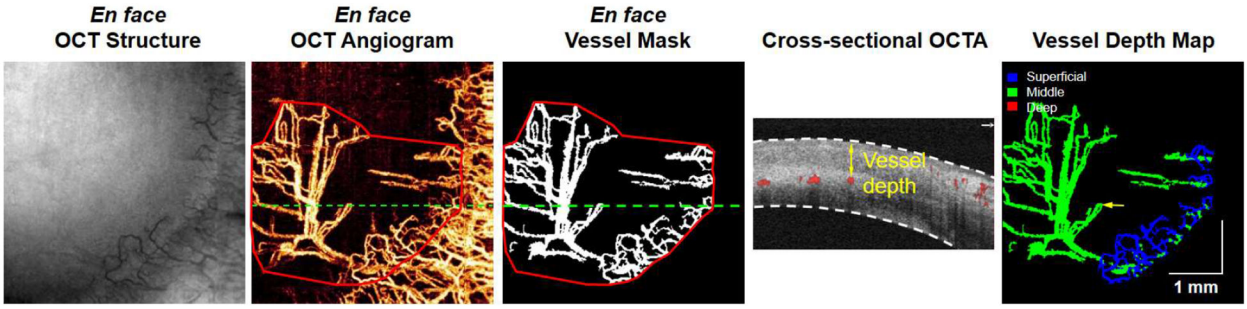

Figure 1.

Corneal neovascularization (NV) vessel density and vessel depth measurements using optical coherence tomography (OCT) and OCT angiography (OCTA). The vessel density was calculated as a percentage of the corneal NV region (delineated by red lines) occupied by vessels (marked by white pixels on the *en face* vessel mask). The vessel density was measured to be 36% in this example. Cross-sectional OCTA shows vessels (projection resolved flow signal in red) within the cornea and conjunctiva (reflectance signal in grayscale). The vessel depth was measured using the distance from anterior corneal surface to the vessel. The percentage vessel depth over corneal thickness was calculated at each vessel location and mapped using different colors: Superficial (anterior 25%, blue), mid-stromal (25~75%, green), or deep (posterior 25%, red). The vessel depth was measured to be 51% at the location marked by yellow arrows. Green dashed lines indicate the levels at which the cross-sectional OCTA was obtained.

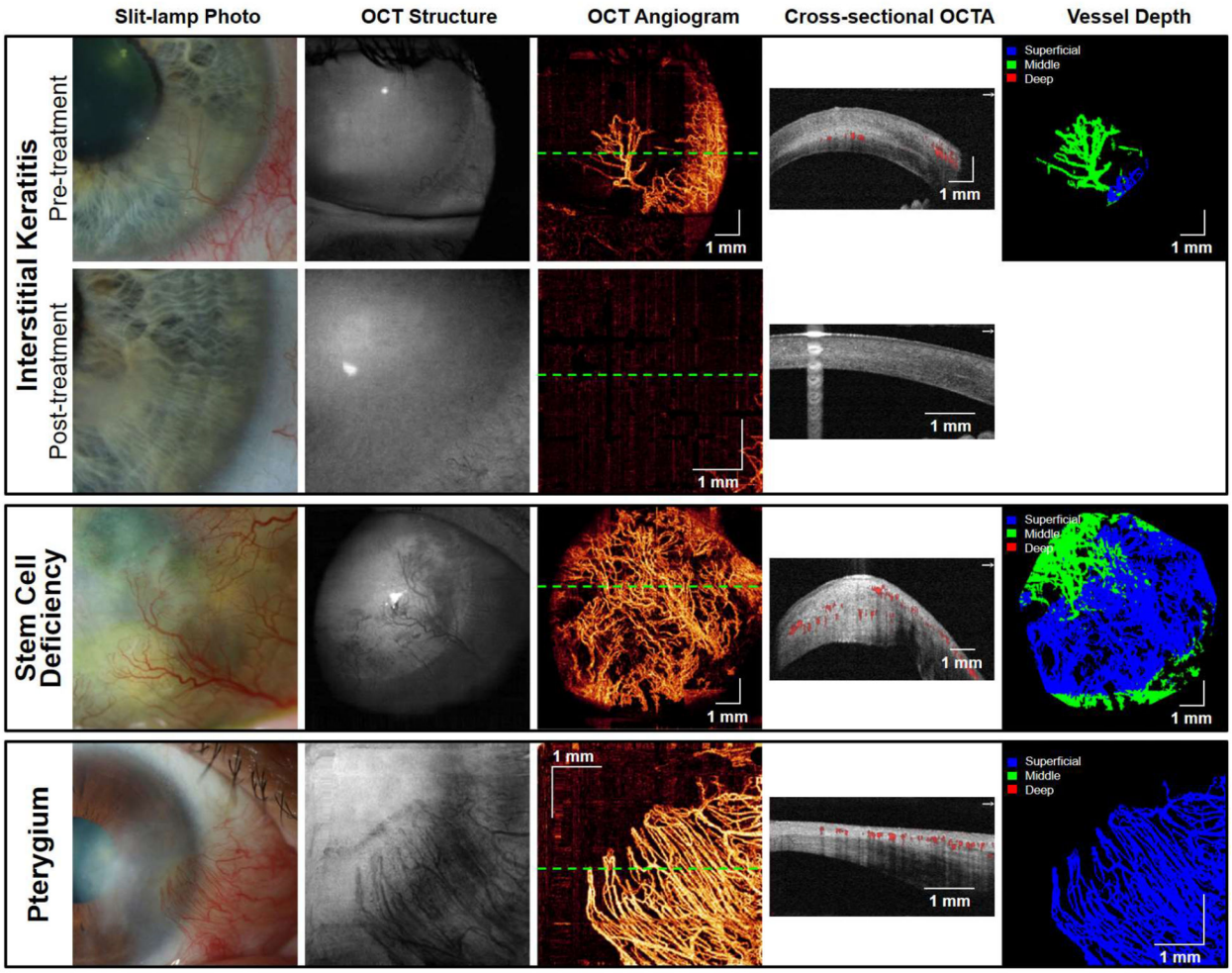

Figure 2.

Corneal OCT and OCT angiography (OCTA) in cases of pathologic neovascularization with an 840-nm spectral-domain system. Top: An interstitial keratitis case before and after treatment. The corneal vessels resolved 1 month after the initiation of topical corticosteroid administration. Middle: A severe limbal stem cell deficiency case with corneal conjunctivalization. Bottom: A pterygium case.

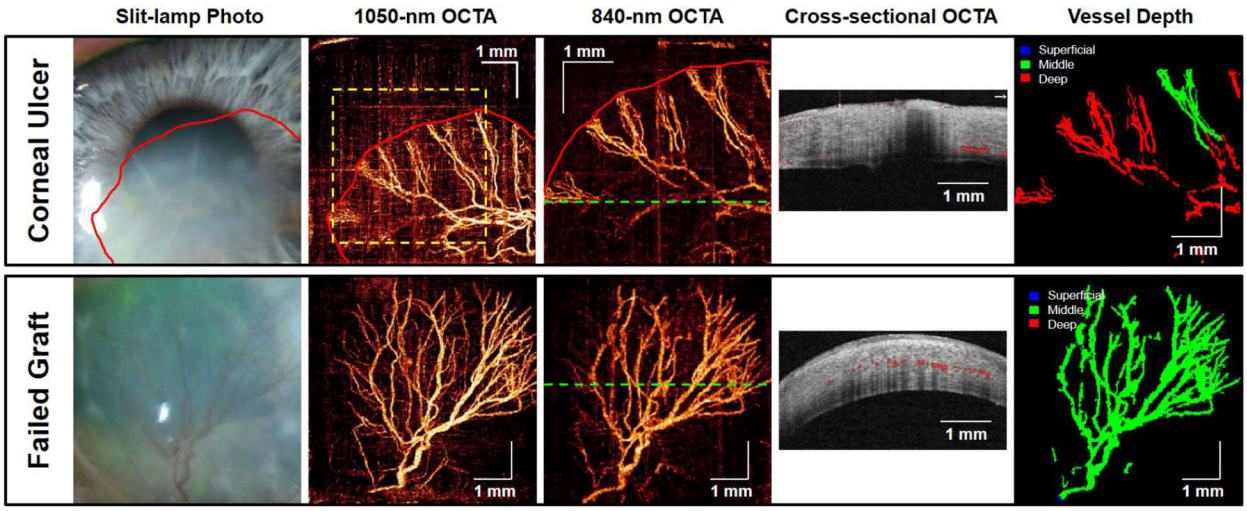

Figure 3:

Comparison of 840-nm spectral-domain versus 1050-nm swept-source corneal OCTA. Top: Corneal NV within a dense stromal scar of a corneal ulcer case, demonstrating improved vessel detection through corneal opacity using longer wavelength 1050-nm OCTA compared to 840-nm OCTA. Bottom: Corneal NV in a failed graft demonstrating similar results using either OCT system.

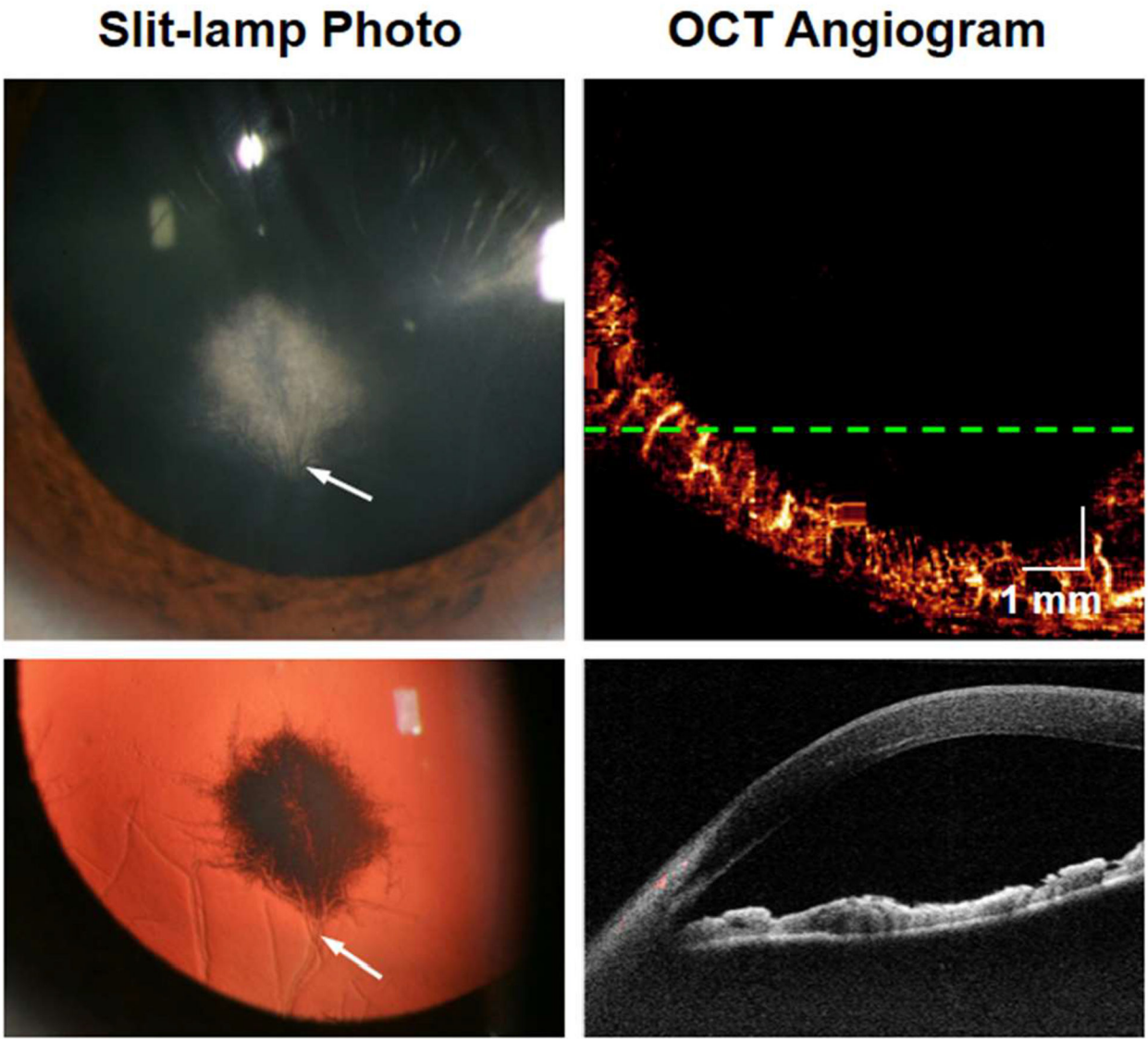

Figure 4:

Ghost vessels (marked by white arrows) evident in the slit-lamp photo of a quiescent herpetic interstitial keratitis case were not imaged using corneal OCTA due to the absence of active blood flow.

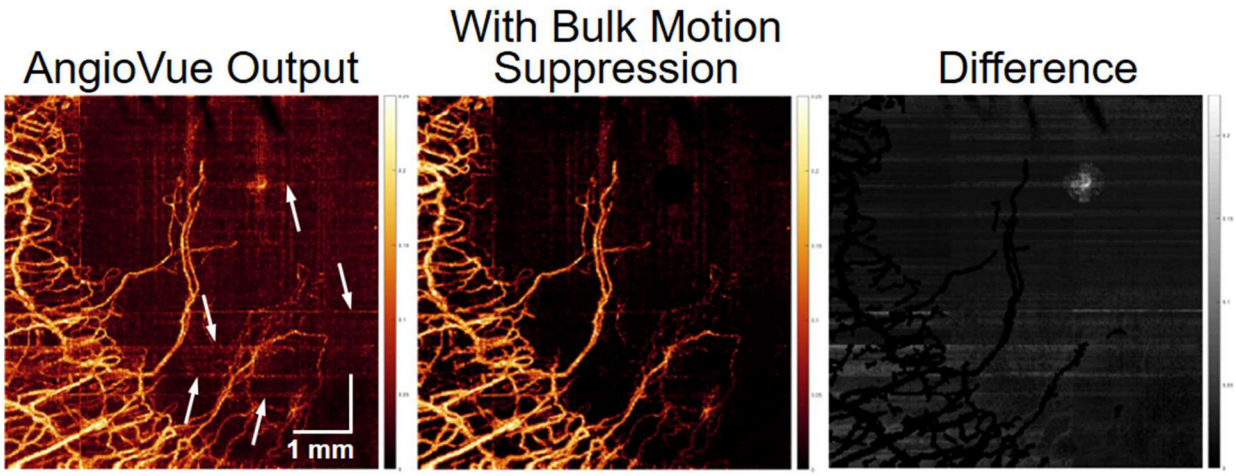

Figure 5:
Corneal OCT angiogram demonstrated that motion artifacts (marked by white arrows) due to eye movement can be effectively reduced using a bulk motion suppression algorithm.